Available online at www.sciencedirect.com
ScienceDirect
Developmental Biology 315 (2008) 280–289
DEVELOPMENTAL BIOLOGY
www.elsevier.com/developmentalbiology

Cripto-independent Nodal signaling promotes positioning of the A–P axis in the early mouse embryo

Giovanna L. Liguori [b,*,1], Ana Cristina Borges [a,c,1], Daniela D'Andrea [b], Annamaria Liguoro [b], Lisa Gonçalves [a,c], Ana Marisa Salgueiro [a,c], M. Graziella Persico [b,1,†], José Antonio Belo [a,c,*,1]

[a] *IBB-Institute for Biotechnology and Bioengineering, Centro de Biomedicina Molecular e Estrutural, Universidade do Algarve, Campus de Gambelas, 8005-135 Faro, Portugal*
[b] *Institute of Genetics and Biophysics "A. Buzzati-Traverso", CNR, Via Pietro Castellino 111, 80131 Naples, Italy*
[c] *Instituto Gulbenkian de Ciência, 2781-901 Oeiras, Portugal*

Received for publication 8 January 2007; revised 4 December 2007; accepted 5 December 2007
Available online 31 December 2007

Abstract

During early mouse development, the TGFβ-related protein Nodal specifies the organizing centers that control the formation of the anterior–posterior (A–P) axis. EGF-CFC proteins are important components of the Nodal signaling pathway, most likely by acting as Nodal coreceptors. However, the extent to which Nodal activity depends on EGF-CFC proteins is still debated. *Cripto* is the earliest EGF-CFC gene expressed during mouse embryogenesis and is involved in both A–P axis orientation and mesoderm formation. To investigate the relation between Cripto and Nodal in the early mouse embryo, we removed the Nodal antagonist *Cerberus 1* (*Cer1*) and simultaneously *Cripto*, by generating *Cer1;Cripto* double mouse mutants. We observed that two thirds of the *Cer1;Cripto* double mutants are rescued in processes that are severely compromised in *Cripto*$^{-/-}$ embryos, namely A–P axis orientation, anterior mesendoderm and posterior neuroectoderm formation. The observed rescue is strongly reduced in *Cer1;Cripto;Nodal* triple mutants, suggesting that Nodal can signal extensively in the absence of Cripto, if *Cer1* is also inhibited. This signaling activity drives A–P axis positioning. Our results provide evidence for the existence of Cripto-independent signaling mechanisms, by which Nodal controls axis specification in the early mouse embryo.

Keywords: Cerberus 1; Cripto; Nodal; Gastrulation; A–P axis; Mouse; Double mutant

Introduction

A signaling pathway centered on Nodal, a member of the Transforming growth factor-β (TGF-β) superfamily, is responsible for crucial events in the configuration of the vertebrate embryo, such as the definition of both anterior–posterior (A–P) and left–right (L–R) axes and the formation of mesoderm and endoderm germ layers (Schier, 2003). In the mouse embryo, the A–P axis becomes explicit during gastrulation with the appearance of the primitive streak, marking the posterior extreme of the embryo (Beddington and Robertson, 1998). However, before the onset of gastrulation, some genes, such as *Cerberus 1* (*Cer1*) and *Lefty1*, begin to be expressed in the distal visceral endoderm (DVE), while other genes, such as *Cripto*, *Brachyury* and *Fgf8*, are specifically expressed in the proximal epiblast (Belo et al., 1997; Beddington, 1998; Beddington and Robertson, 1998, 1999; Ding et al., 1998; Yamamoto et al., 2004). This gene expression asymmetry defines a proximal–distal (P–D) polarity inside the mouse embryo, before gastrulation (Beddington, 1998; Beddington and Robertson, 1998, 1999). Later, the DVE cells migrate asymmetrically toward the prospective anterior side of the egg cylinder, giving rise to the anterior visceral endoderm

* Corresponding authors. J.A. Belo is to be contacted at IBB-Institute for Biotechnology and Bioengineering, CBME/FERN, Universidade do Algarve, Campus de Gambelas, 8005-139 Faro, Portugal. Fax: +351 289 818 419. G.L. Liguori, Institute of Genetics and Biophysics "A. Buzzati-Traverso", CNR, Via Pietro Castellino 111, 80131 Naples, Italy. Fax: +39 081 6132 595.
E-mail addresses: liguori@igb.cnr.it (G.L. Liguori), jbelo@ualg.pt (J.A. Belo).
† Deceased 5 February 2007.
[1] These authors contributed equally to this work.

0012-1606/$ - see front matter © 2007 Elsevier Inc. All rights reserved.
doi:10.1016/j.ydbio.2007.12.027

(AVE); in the meantime, the expression of the proximal genes is restricted to the posterior embryonic pole, which will give rise to the primitive streak (Ang and Constam, 2004; Beddington, 1998; Beddington and Robertson, 1998, 1999). The unilateral migration of the DVE converts the P–D to an A–P axis, presumably by directing cell movements and regulating gene expression in the epiblast (Ang and Constam, 2004; Perea-Gomez et al., 2002; Yamamoto et al., 2004).

Nodal is required both to specify the DVE, which moves anteriorward to form the AVE, and to pattern the epiblast (Lu and Robertson, 2004). In fact, *Nodal* null mutants fail to form a P–D axis (Brennan et al., 2001; Conlon et al., 1994). Later on, Nodal signaling provides the driving force for DVE migration and thus promotes the conversion of the initial P–D polarity into the A–P axis (Yamamoto et al., 2004). Nodal signaling depends upon interaction with EGF-CFC cofactors and Activin type I and II receptors (ActRI and II) (reviewed in Schier, 2003; Shen, 2007; Whitman, 2001). Nodal activity is also tightly limited in space and time by inhibitory factors, such as Cer1, Tomoregulin, Drap1, Lefty1 and Lefty2 (reviewed in Schier, 2003; Shen, 2007; Whitman, 2001). The EGF-CFC founder member Cripto, together with the Nodal antagonists Cer1 and Lefty1, directs the proper orientation of the A–P axis, and gastrulation movements (Ding et al., 1998; Xu et al., 1999; Liguori et al., 2003; Perea-Gomez et al., 2002; Yamamoto et al., 2004). In fact, *Cripto* null mutants fail to convert the initial P–D into an A–P axis and also fail to form embryonic mesoderm (Ding et al., 1998; Liguori et al., 2003). This phenotype is striking, because *Cripto* expression has never been detected in the visceral endoderm (reviewed in Shen and Schier, 2000). Moreover, analysis of chimeras consisting of wt epiblast and *Cripto*$^{-/-}$ extraembryonic tissues clearly demonstrates that *Cripto* is not essential in visceral endoderm (Kimura et al., 2001). On the other side, Cer1 and Lefty1 synergistically act to determine the direction of migration of the DVE cells (which define the future anterior pole of the embryo) as well as to restrict primitive streak formation in the embryo to the posterior pole (Perea-Gomez et al., 2002; Yamamoto et al., 2004).

The EGF-CFC molecules are membrane-attached extracellular proteins, found only in vertebrates (Persico et al., 2001; Shen and Schier, 2000). Family members have been characterized in mouse (Cripto and Cryptic), human (CRIPTO and CRYPTIC), chick (Cripto), zebrafish (one-eyed pinhead [oep]) and frog (FRL-1) (Persico et al., 2001; Shen and Schier, 2000). Biochemical studies indicate that Cripto and Cryptic form a complex with Nodal, ActRIB (ALK4) and ActRIIB (Reissman et al., 2001; Yeo and Whitman, 2001; Whitman, 2001). Mechanistically, EGF-CFC factors appear to function as co-receptors, enhancing Nodal binding to the type I/II receptor complex. However, the extent to which Nodal activity depends on EGF-CFC proteins remains unresolved. On the one hand, *in vitro* studies show that Cripto interaction with ALK4 is necessary both for Nodal binding to the ALK4/ActRIIB receptor complex and for Smad2 activation by Nodal (Yeo and Whitman, 2001). Studies in zebrafish also suggest that EGF-CFCs are absolutely required for Nodal signaling, since Nodal has no apparent effect on *oep* mutants (Gritsman et al., 1999). Moreover, Vg1 and Gdf1 signaling in zebrafish also depends on EGF-CFCs proteins, suggesting that multiple TGF-β signals converge on ActR/EGF-CFC complexes (Cheng et al., 2003). On the other hand, cell culture assays indicate that Nodal signaling via the ActRIA (ALK7) receptor is enhanced by EGF-CFC proteins but does not absolutely require them (Reissman et al., 2001). In addition, the mouse *Cripto* null mutation does not precisely phenocopy the *Nodal* loss of function. In particular, the *Nodal*$^{-/-}$ mouse embryo is not able to specify an A–P axis (Conlon et al., 1994), whereas in *Cripto* null mutants, the rudiment of an A–P axis is recognizable, even though it is not correctly oriented (Ding et al., 1998; Liguori et al., 2003). Recent experiments have also shown that unprocessed Nodal pro-protein is able to bind both ALK4 and ActRIIB receptors in transfected 293T cells, even though neither Cripto nor other EGF-CFC factors are co-transfected (Ben-Haim et al., 2006). The purified recombinant Nodal pro-protein is also able to induce *Bmp4* and *PACE4* expression in mouse extraembryonic ectoderm explants, although neither *Cripto* nor *Cryptic* genes are expressed in extraembryonic ectoderm (Ding et al., 1998; Kimura et al., 2001; Shen et al., 1997); this activity has been shown to be ALK4-dependent (Ben-Haim et al., 2006). Cripto is also able to act non cell autonomously both *in vitro* in cell coculture assays and *in vivo* during mouse embryogenesis (Yan et al., 2002; Chu et al., 2005). These data suggest that Cripto can also function in trans as an intercellular mediator of Nodal signaling activity (Chu et al., 2005). Finally, Cripto is thought to promote tumor growth via Nodal-independent mechanisms, such as activation of a ras/raf/MAP kinase pathway or inhibition of TGF-β and Activin signaling (Bianco et al., 2003; Adkins et al., 2003; Gray et al., 2003, 2006; Strizzi et al., 2005). In summary, both Nodal and Cripto are multifunctional signaling proteins, involved in numerous physiological and pathological processes. Therefore, the relation between Cripto and Nodal constitutes a crucial point for the reciprocal regulation of their activity and this relation needs further characterization.

To investigate the extent to which Cripto is required for Nodal signaling in the mouse embryo, we designed a double mutant mouse strategy, taking advantage of both *Cripto* and *Cer1* null mutants (Belo et al., 2000; Liguori et al., 2003). Cer1 is a Nodal inhibitor that antagonizes Nodal by direct interaction in the extracellular space (Belo et al., 2000). Therefore, the removal of Cer1 should increase the level of free Nodal ligand, by releasing Nodal from Cer1 inhibition. If Cripto is absolutely required for Nodal signaling, this increase in Nodal level should have no effect, and the *Cer1;Cripto* double mutants should have the same phenotype as *Cripto* null mutants. Alternatively, if the increased level of Nodal protein can bypass Cripto function, the outcome would be a rescue of the *Cripto*$^{-/-}$ early lethal phenotype. We chose Cer1 from among the different Nodal antagonists for two important reasons. First of all, Cer1 exerts its action without interacting with Cripto (in contrast, Lefty1, Lefty2 and Tomoregulin antagonize Nodal signaling by blocking Cripto and preventing the formation of the receptor complex; Chen and Shen, 2004; Cheng et al., 2004; Harms and Chang, 2003). Secondly, the

Cer1 null mutation produces no evident phenotype in the mouse embryo (Belo et al., 2000); hence, the *Cer1;Cripto* double mutants need only to be compared with Cripto-deficient embryos, greatly simplifying our analysis.

Here we show that the removal of the Nodal antagonist *Cer1* does indeed partially rescue the mouse *Cripto*$^{-/-}$ phenotype. *Cer1;Cripto* compound mutants recover the orientation of the A–P axis and most of the subsequent gastrulation processes, which are severely impaired in the *Cripto* null mutants. Moreover, a subset of *Cer1*$^{-/-}$*;Cripto*$^{-/-}$ embryos show the formation of a double axis. All together, these data demonstrate that Cer1 and Cripto genetically interact in mouse to control embryonic axis development. The rescue of the expression of Nodal target genes observed in *Cer1;Cripto* mutants indicates the recovery of Nodal signaling, which is severely compromised in *Cripto*$^{-/-}$ embryos. Accordingly, the *Cer1;Cripto* rescued phenotype is impaired if we genetically reduce *Nodal* strength. Our results demonstrate that, in *Cripto*$^{-/-}$ mutants, partial recovery of Nodal signaling is achieved by inactivating the *Cer1* gene. In summary, this work shows for the first time that in the mouse embryo a Cripto-independent Nodal signaling is able to position the A–P axis correctly and to form both anterior mesendoderm and posterior neuroectoderm.

Experimental procedures

Generation and genotyping of compound mutants

Cer1$^{-/-}$ mice (Belo et al., 2000) were crossed to *Cripto*$^{+/-}$ heterozygous mice (Xu et al., 1999) (both on a C57BL/6 background) to provide double heterozygotes. The *Cer1*$^{+/-}$*;Cripto*$^{+/-}$ mice were later crossed to *Cer1*$^{-/-}$ mice to generate *Cer1*$^{+/-}$*;Cripto*$^{+/-}$ as well as *Cer1*$^{-/-}$*;Cripto*$^{+/-}$ animals. The *Cer1*$^{-/-}$*;Cripto*$^{+/-}$ mice were intercrossed to collect *Cer1*$^{-/-}$*;Cripto*$^{-/-}$ embryos as well as crossed to *Cripto*$^{+/-}$ mice to obtain the *Cer1*$^{+/-}$*;Cripto*$^{-/-}$ embryos. For the triple mutant experiments, *Cer1*$^{+/-}$*;Cripto*$^{+/-}$ mice were crossed to *Nodal*$^{+/-}$ heterozygotes (Lowe et al., 2001) to generate *Cer1*$^{+/-}$;*Cripto*$^{+/-}$;*Nodal*$^{+/-}$ mutants. Those were then crossed with *Cer1*$^{-/-}$;*Cripto*$^{+/-}$ animals to produce both *Cer1*$^{+/-}$*;Cripto*$^{-/-}$;*Nodal*$^{+/-}$ and *Cer1*$^{-/-}$;*Cripto*$^{-/-}$;*Nodal*$^{+/-}$ embryos. Noon of the day on which the vaginal plug was detected was considered as 0.5 dpc. Procedures conform to regulations protecting animals used for research purposes, including those of the DL 116/92 (Italy) and DL 129/92, Portaria 1005/92 (Portugal).

For genotyping of adult mice, DNA was extracted from tail tips as previously described (Yamamoto et al., 2004) and then analyzed by means of PCR, using *Cer1* (Belo et al., 2000), *Cripto* (Xu et al., 1999) and *Nodal* (Lowe et al., 2001) specific primers. Embryos were first analyzed by whole-mount *in situ* hybridization (WISH) and later genotyped by PCR. Whole embryos at 6.7–7.5 dpc or half embryos at 8.5 dpc were digested in 20 µl of Lysis Buffer using 1 mg/ml of proteinase K, according to the protocol previously described (Xu et al., 1999). The PCR protocol was the same used for the adult tail DNA, with the only difference that 40 cycles instead of 30 were applied.

Whole-mount in situ hybridization and histology

WISH experiments were performed as previously described (Liguori et al., 2003). Two color *in situ* hybridization was done with one RNA probe labeled with Digoxigenin (Roche) and the other with Fluorescein (Roche) according to standard protocols. After development of the first probe with NBT/BCIP (Roche), alkaline phosphatase was inactivated by a methanol series and the second probe was developed with INT/BCIP (Roche). Detailed descriptions on the RNA probes and constructs are available from the authors upon request. The embryos were then photographed using a Leica DFC320 digital camera, and subsequently digested and genotyped by PCR. Some embryos were embedded in 7.5% gelatine, frozen, sectioned using a Leica CM3050 S cryostat, and then examined and photographed using a Leica DM LB2 microscope and a Leica DFC320 digital camera.

Results and discussion

Cer1$^{-/-}$*;Cripto*$^{-/-}$ *embryos form an A–P axis*

We generated *Cer1;Cripto* mouse double mutants by crossing *Cer1*$^{-/-}$ (Belo et al., 2000) and *Cripto*$^{+/-}$ (Liguori et al., 2003) mice. The resulting *Cer1*$^{-/-}$*;Cripto*$^{+/-}$ are apparently normal and fertile and were intercrossed to collect double null mutants to compare with *Cripto*$^{-/-}$ embryos.

We began by analyzing embryos at 8.5 days post coitum (dpc) by whole-mount antisense mRNA *in situ* hybridization (WISH; Fig. 1). At this stage, *Cripto*$^{-/-}$ mutants are smaller than wild-type (wt) embryos, show a severely compromised embryonic region and form neural territories only anterior to the *Gbx2* expression domain; in particular, expression of more caudal markers (*Krox20*, *HoxB1* and *HoxB4*) is never observed (Ding et al., 1998; Liguori et al., 2003). Moreover, the neural territories do not develop along an A–P but along a P–D axis (Figs. 1e–g; Liguori et al., 2003). In contrast, 70% of the double null mutants express *Krox20* which identifies rhombomeres 3 and 5 of the posterior hindbrain (Fig. 1j). In addition, 70% of the *Cer1*$^{-/-}$*;Cripto*$^{-/-}$ embryos ($n=10$) express *Krox20* and the other neural markers analyzed, including *Otx2* (forebrain and midbrain), *Gbx2* (anterior hindbrain) and *Wnt1* (dorsal midbrain) along an A–P axis (Figs. 1i–k) as in the wt embryo (Figs. 1a–c), not along a P–D axis as in the Cripto null mutants (Figs. 1e–g). Interestingly, we also found that 20% ($n=10$) of the double null mutants analyzed at 8.0–8.5 dpc form a secondary anterior neuraxis, revealed by the expression of both *Otx2* and *Wnt1* genes (Figs. 1m–p). In contrast, *Shh* is expressed in a few cells close to the extremity of only one of the two axes (Fig. 1p). A similar phenotype has been previously described in the *Cer1*$^{-/-}$*Lefty1*$^{-/-}$ mutants in which two Nodal inhibitors are inactivated (Perea-Gomez et al., 2002). However, while *Cer1*$^{-/-}$*;Lefty1*$^{-/-}$ embryos also duplicate trunk structures, the *Cer1*$^{-/-}$*;Cripto*$^{-/-}$ mutants show a normal trunk with a node and notochord (Fig. 1o).

At 9.5 dpc, *Cripto*$^{-/-}$ mutants consist primarily of extra-embryonic tissue (Fig. 1h); by 10.5 dpc, they are reabsorbed (Xu et al., 1999). In contrast, double null mutants can be found at 9.5 dpc, in which the embryonic region is well developed and clearly shows an A–P axis, with a head that expresses *Otx2* and a morphologically distinguishable allantoid-like structure on the opposite side (Fig. 1l). These double null mutants appear delayed, resembling 8.0–8.2 dpc (Fig. 1m) rather than 9.5 dpc (Fig. 1d) wt embryos, but nonetheless are significantly different from *Cripto*$^{-/-}$ mutants, in which no morphological structure is recognizable. *Shh* expression, although defective, is detected in the embryo midline (Fig. 1l). Strikingly, at 12.5 dpc *Cer1*$^{-/-}$*;Cripto*$^{-/-}$ embryos can still be identified (Figs. 1s–u). Half of the surviving *Cer1*$^{-/-}$*;Cripto*$^{-/-}$ embryos ($n=6$) are an almost empty yolk sac, but the other half develops the major embryonic axes with distinct head, trunk and tail structures (Figs. 1s–u).

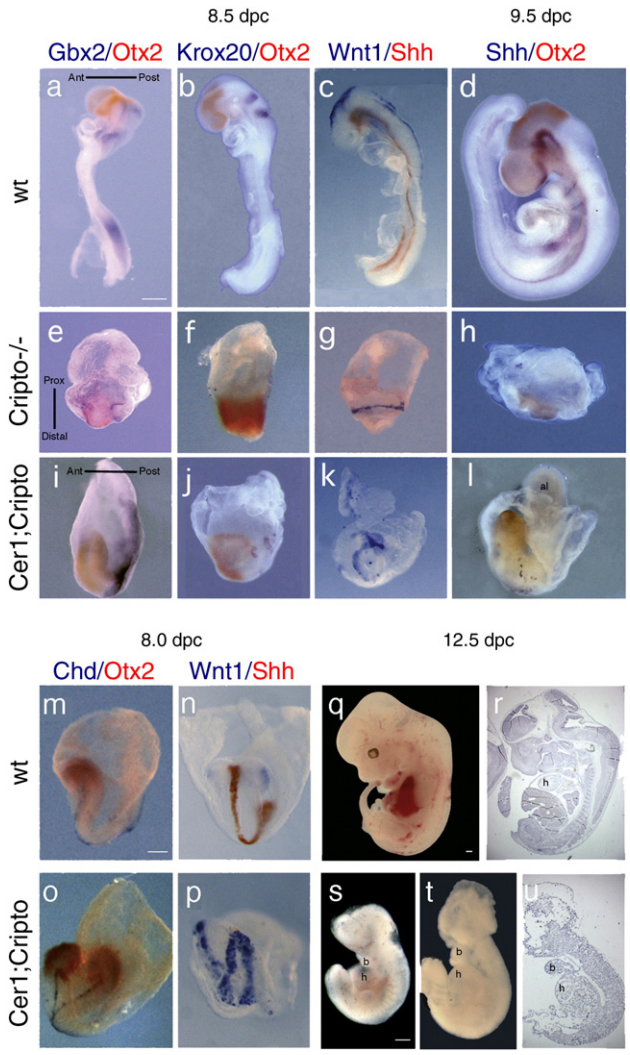

Fig. 1. Rescue of posterior neuroectoderm and trunk structures in *Cer1;Cripto* double mutant embryos. (a–p) Molecular analysis by double whole-mount *in situ* hybridization (WISH) of 8.5 (a–c, e–g, i–k) and 9.5 dpc (d, h, l) wild-type (wt) (a–d), *Cripto*$^{-/-}$ (e–h) and *Cer1*$^{-/-}$*;Cripto*$^{-/-}$ embryos (i–l). a, e, i, in the *Cripto* null mutants (e), *Otx2* (red) and *Gbx2* (blue) are expressed along a P–D axis whereas in the *Cer1*$^{-/-}$*;Cripto*$^{-/-}$ double mutants (i) the expression domains are aligned along an A–P axis, as in the wt embryo (a). b, f, j, in the *Cripto*$^{-/-}$ embryos (f), the marker of the rhombomeres 3 and 5 *Krox-20* is not expressed, in contrast to the double null mutants (j). Concomitantly, *Otx2* expression domain is anteriorized in double mutants. c, g, k, in the *Cripto* null mutants (g), the expression of *Wnt1* (blue) is radial while in the double null mutants (k), *Wnt1* expression is oriented along the A–P axis. The expression of the ventral neural marker *Shh* (red) is not rescued. d, h, i, *Cripto*$^{-/-}$ embryos (h) have almost completely degenerated, although retain *Otx2* expression. In contrast, the double mutants (i) display an embryonic axis, even if reduced respect to the wt embryos (d), with *Otx2* domain in one of the extremities and patches of *Shh* expression along the midline. m-p, double WISH of 8.0 dpc wt (m, n) and *Cer1*$^{-/-}$*;Cripto*$^{-/-}$ embryos (o, p), analyzed for *Chordin* and *Otx2* (m, o) and for *Wnt1* and *Shh* (n, p). In some double null mutants, we observed duplication of the embryonic axis (o, p). (q–u) Morphological analysis of 12.5 dpc wt (q, r) and *Cer1*$^{-/-}$*;Cripto*$^{-/-}$ (s–u) embryos. (r, u) Parasagittal sections of the wt embryo in q (r) and of the *Cer1*$^{-/-}$*;Cripto*$^{-/-}$ embryo in t (u). The *Cer1*$^{-/-}$*;Cripto*$^{-/-}$ embryos are significantly smaller than the wt embryos, show anterior head truncations, but form branchial arches and a rudimentary heart. The direction of the axes is shown. Abbreviations Ant: anterior; al: allantoid-like structure; b: branchial arch; h: heart; Post: Posterior; Prox: Proximal. Scale bars represent 300 μm.

The presence of posterior neuroectoderm and a developing heart in the double mutants is remarkable, since these structures are completely absent in *Cripto* null single mutants (Ding et al., 1998; Liguori et al., 2003).

To investigate the effects of inactivating a single *Cer1* allele, we crossed the *Cer1*$^{-/-}$*;Cripto*$^{+/-}$ mice to *Cripto*$^{+/-}$ mice to obtain *Cer1*$^{+/-}$*;Cripto*$^{-/-}$ embryos. We analyzed the *Cer1*$^{+/-}$*;Cripto*$^{-/-}$ mutants at both 8.5 and 9.5 dpc ($n=10$) for the expression of the markers described above. *Cer1*$^{+/-}$*;Cripto*$^{-/-}$ embryos also develop an A–P axis (60%; data not shown), essentially like the *Cer1*$^{-/-}$*;Cripto*$^{-/-}$ mutants. Thus, the removal of *Cer1*, even one of the two gene copies, rescues significant features of the *Cripto*$^{-/-}$ phenotype. In summary, we show that double mutant embryos clearly develop further than *Cripto*$^{-/-}$ mutants; in particular, they form posterior neuroectoderm and correctly position the A–P axis. These data demonstrate that *Cer1* and *Cripto* genetically interact in mouse to control embryonic axis development.

The removal of Cer1 rescues gastrulation defects of Cripto$^{-/-}$ *embryos*

By analysis of earlier embryonic stages, we observed that gastrulation is less impaired in the *Cer1*$^{-/-}$*;Cripto*$^{-/-}$ mutants than in *Cripto*$^{-/-}$ embryos. At these early stages, we found no significant differences between *Cer1*$^{+/-}$*;Cripto*$^{-/-}$ and *Cer1*$^{-/-}$*;Cripto*$^{-/-}$ embryos, and therefore both genotypes are included in our analysis (samples referred to as double or *Cer1;Cripto* mutants). At 7.5 dpc, concomitant with the reduction and anteriorization of the *Otx2* expression domain (Figs. 2c, d, k, l), the double mutants also develop trunk structures (Figs. 2c, d, g, h, k, l), which are not formed in *Cripto*$^{-/-}$ embryos (Figs. 2b, f, j). *Brachyury* expression domain, which identifies the primitive streak (PS) and the forming mesoderm (Fig. 2a), is enlarged in 60% ($n=10$) of the double mutants (Fig. 2c) compared to the *Cripto*$^{-/-}$ embryos (Fig. 2b). In 20% of the double mutants, *Brachyury* expression also extends toward the distal tip of the embryo (Fig. 2d). The analysis at 7.5 dpc revealed that 69% ($n=23$) of the double mutants also express other markers that are completely absent in the *Cripto*$^{-/-}$ embryos, for example *Lim1*, which identifies the PS and mesodermal wings and later the node and axial mesoderm (Figs. 2e–h), *Foxa2*, expressed in the node, the midline and anterior definitive endoderm (Figs. 2e–h), and *Chordin* (*Chd*), which marks the node and the axial mesendoderm (Figs. 2i–l). In agreement with previous data, at 6.7 dpc 60% ($n=23$) of the compound, mutants rescue the expression of AVE markers like *Dkk* and *Lim1* in the anterior of the VE (Figs. 2m–r), and also of the PS marker *Fgf8* in the posterior of the epiblast (Figs. 2p–r). We also detected the expression of *Wnt3*, marking both posterior epiblast and visceral endoderm in the wt embryo (2t). In both *Cripto* single mutants and *Cer1;Cripto* double mutants, *Wnt3* expression is weaker than in wt embryo (Figs. 2t–w); however, in the 67% of double mutants ($n=3$), *Wnt3* expression domain is shifted posterior, as in the wt, while in the *Cripto*$^{-/-}$ embryos, expression stays proximal. Moreover, double mutant embryos express the anterior PS marker *Foxa2*, which is never detected in the

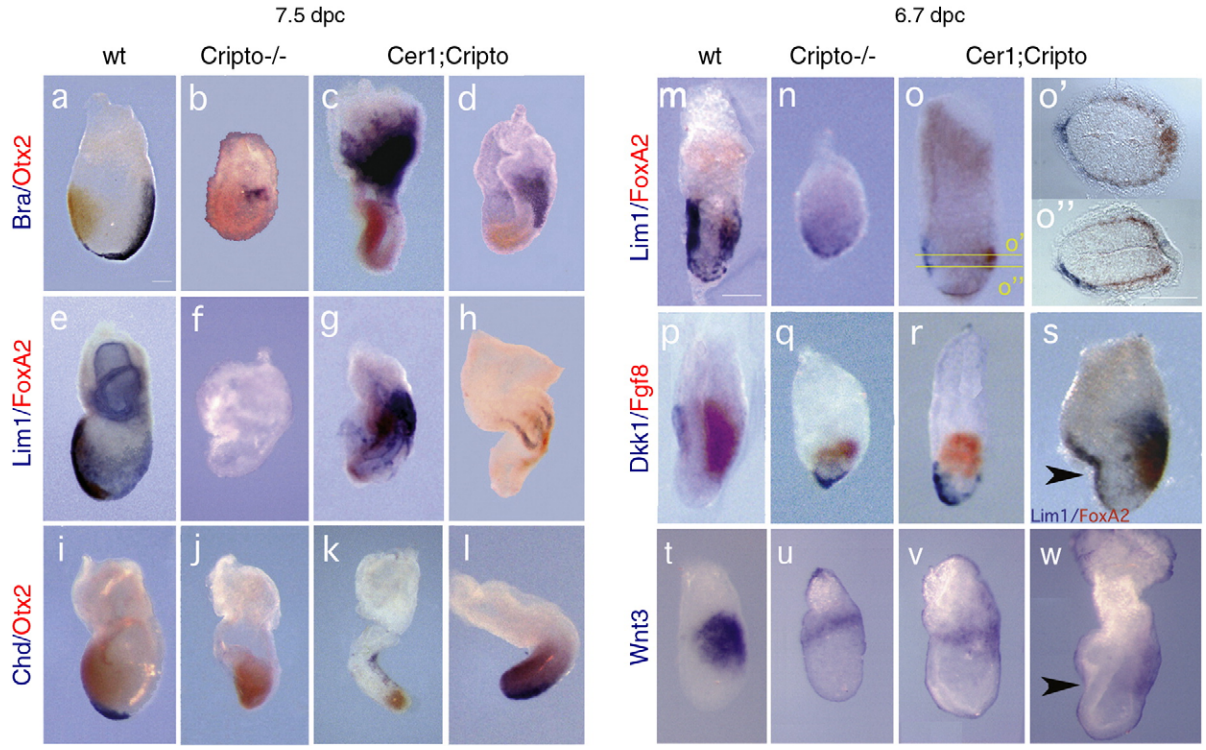

Fig. 2. *Cer1;Cripto* double mutants display rescue of AVE rotation, primitive streak elongation and node derivatives. Molecular analysis by whole-mount double *in situ* hybridization of 7.5 (a–l) and 6.7 dpc (m–w) wild-type (wt) (a, e, i, m, p, t), *Cripto*$^{-/-}$ (b, f, j, n, q, u) and *Cer1;Cripto* double mutant embryos (c, d, g, h, k, l, o, r, s, v, w). (a–d) The *Otx2*(red) domain is anteriorized in the double mutants (c, d) compared to *Cripto*$^{-/-}$ embryos (b), whereas *Brachyury* (blue) expression is enlarged (c) and in some double mutants the primitive streak extends toward the distal tip (d). (e–h) *Lim1* (blue) and *Foxa2* (red) are never detected in *Cripto*$^{-/-}$ embryos (f) in contrast to the double mutants (g, h), indicating that a primitive streak, the node and its derivatives are present. (i–l) *Chordin* (blue) expression revealed that in the double mutants (k, l) the node and axial mesendoderm are present in contrast to the complete absence in the *Cripto* null mutants (j). (m–o, s) *Lim1* (blue) and *Foxa2* (red) also revealed a correct localization of the A–P axis in the double mutant embryos (o), even though in some cases a constriction in the anterior embryonic region can be observed (s). (o′, o″) Cross sections of the embryo shown in o, at the indicated levels, showing the formation of the primitive streak and the AVE rotation toward the anterior side. (p–r) In the double mutants (r), *Dkk* (blue) expression domain is more anterior and *Fgf8* (red) expression more distal than in *Cripto*$^{-/-}$ embryos (q). (t–w) In the *Cripto*$^{-/-}$ embryos, *Wnt3* expression is fainter than in the wt embryos and located in the proximal region of the embryo (u). In the *Cer1;Cripto* mutants, Wnt3 expression remains as weak as in the *Cripto*$^{-/-}$ mutants, but is while is located more posterior (v, w), resembling the wt embryos (t). Arrowheads indicate the constriction in the anterior region of double mutants. Scale bars represent 180 μm.

Cripto null mutants (Figs. 2p–s). We note that a small percentage of double null mutants (9%, $n=23$) show a peculiar characteristic: a marked bend or constriction in the anterior region (Figs. 2s, w).

Collectively, these data confirm and extend the conclusions reported above that the double mutants have a milder phenotype than the *Cripto*$^{-/-}$ embryos. At 6.7 dpc, double mutants have completely converted or are beginning to convert the initial embryonic P–D asymmetry to an A–P axis (Figs. 2o, r) resembling wt embryos (Figs. 2m, p). By contrast, this axis conversion process is completely abolished in *Cripto*$^{-/-}$ embryos (Figs. 2n, q) (Ding et al., 1998; Liguori et al., 2003). At later stages, the double mutants form not just posterior and extraembryonic mesoderm (as *Cripto*$^{-/-}$ embryos) but also more anterior and later structures, such as the node and its derivatives including the axial mesendoderm (Figs. 2g, h, k, l).

Cer1;Cripto mutants rescue Nodal signaling

Cer1;Cripto double mutants appear rescued in most of the biological processes that are controlled by Nodal. In fact, *Cer1;Cripto* embryos share many phenotypic characteristics with mutants in which Nodal signaling is only reduced, such as Nodal hypomorphs (Lowe et al., 2001), asymmetric intronic enhancer (ASE) mutants (Norris et al., 2002) and double mutants for ActRIIA and ActRIIB (Song et al., 1999). In order to confirm that Nodal signaling remains active in the *Cer1;Cripto* double mutants, we examined the expression of *Lefty1* and *Lefty2* genes, which mark the AVE and the nascent mesoderm, respectively, and are immediate Nodal responsive genes (Fig. 3a; Meno et al., 1997). At 5.5–5.7 dpc, *Cripto*$^{-/-}$ embryos do not express at all *Lefty1* gene (Fig. 3b), while a very faint *Lefty1* expression is detectable in 2 out of 3 *Cer1;Cripto* mutants (Fig. 3c). At 6.7 dpc, the expression of both *Lefty1* and *Lefty2* genes is not detected in *Cripto*$^{-/-}$ embryos (Fig. 4b) even though the visceral endoderm and nascent mesoderm are present (Figs. 2n, q; Ding et al., 1998). In contrast, we observed that 60% ($n=10$) of the double mutants express *Lefty* genes; in about 20% ($n=10$) of these embryos, the expression domains are also correctly localized, almost resembling a wt embryo (Fig. 4c). We also detected the expression of the *Nodal* gene itself, which is controlled by an autoregulatory loop (Varlet et

al., 1997). At 5.5–5.7 dpc, *Nodal* is expressed in almost all the epiblast of the wt embryo (Fig. 3d). We found that *Cripto*$^{-/-}$ embryos express Nodal just in few cells in the proximal region of the epiblast (Fig. 3e), while in 2 out of 3 *Cer1;Cripto* mutants Nodal expression resembles the expression in the wt embryo (Figs. 3d, f). At 6.7 dpc, *Nodal* is expressed in the posterior epiblast of the wt embryo (Figs. 4d, d') but only in a proximal ring of epiblast cells in the *Cripto*$^{-/-}$ embryo (Figs. 4e, e'). In contrast, almost 57% ($n=7$) of the *Cer1;Cripto* double mutants ectopically express *Nodal* throughout all the embryonic region (Figs. 4f, f'). All together, these results indicate that Nodal signaling remains active in the *Cer1;Cripto* double mutant embryos and is most likely responsible for the rescue observed. To confirm this, we performed an experiment in which *Nodal* gene dosage is diminished. To this purpose, we crossed the *Cer1*$^{+/-}$*;Cripto*$^{+/-}$ double heterozygotes with *Nodal*$^{+/-}$ mice (Lowe et al., 2001). The resulting *Cer1*$^{+/-}$*;Cripto*$^{+/-}$*;Nodal*$^{+/-}$ triple mutants were backcrossed to *Cer1*$^{+/-}$*;Cripto*$^{+/-}$ mice to obtain both *Cer1*$^{-/-}$*;Cripto*$^{-/-}$*;Nodal*$^{+/-}$ and *Cer1*$^{+/-}$*; Cripto*$^{-/-}$*;Nodal*$^{+/-}$ embryos. The embryos were collected between 8.5 and 9.0 dpc and analyzed by double WISH for the expression of *Otx2* and *Krox20*. We chose *Krox20* as an informative marker because it is expressed in the double mutants but is never expressed in *Cripto*$^{-/-}$ embryos. *Otx2* was used as control marker. We observed that only 25% ($n=20$) of the triple mutants express *Krox-20*, in contrast to the 59% ($n=78$) of the double mutants (Figs. 4g–j, Table 1). These data indicate that the *Cer1;Cripto;Nodal* triple mutants have a more defective phenotype than the *Cer1;Cripto* double mutants. Thus, the reduction of Nodal dosage counteracts the phenotypic rescue found in the double mutants, clearly indicating that Nodal signaling plays a crucial role during the embryonic development of *Cer1;Cripto* mutants. Collectively, our data point to the ability of Nodal to signal in the absence of Cripto to mediate both the orientation of the A–P axis and most gastrulation processes.

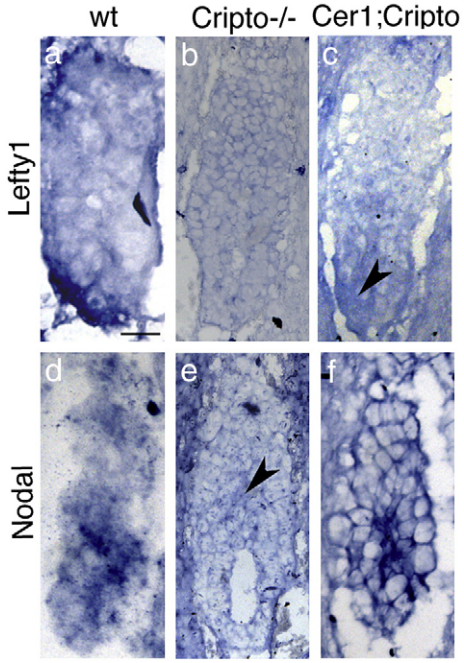

Fig. 3. *Cer1;Cripto* double mutants rescue *Lefty1* and *Nodal* expression before gastrulation. Molecular analysis by whole-mount *in situ* hybridization (WISH) of 5.5–5.7 dpc wild-type (wt) (a, d), *Cripto*$^{-/-}$ (b, e) and *Cer1;Cripto* (c, f). In the wt embryo, *Lefty1* is detected in the distal VE that moves toward the anterior side of the embryo (a). *Cripto*$^{-/-}$ embryos lack expression of *Lefty1* (b), while *Cer1;Cripto* embryos show a faint *Lefty1* expression, marked by the arrowhead. *Nodal* is expressed in almost all the epiblast of the wt embryo (d) while it is detected only in a proximal cluster of epiblast cells (arrowhead) of the *Cripto*$^{-/-}$ embryos (e). Nodal expression in the *Cer1;Cripto* double mutants (f) resembles the expression on the wt embryo (d). Scale bars represent 50 μm.

Cryptic and Alk7 expression profiles argue against a compensatory role of these factors in Cer1;Cripto embryos

We also investigated the expression of two other genes involved in the Nodal pathway: *Cryptic*, the second EGF-CFC gene present in mouse (Shen et al., 1997), and *Alk7*, the only known Nodal receptor whose activity is diminished but not abolished in the absence of Cripto (Reissman et al., 2001). However, *Cryptic* and *Alk7* null mutants do not show embryonic lethality and A–P defects (Yan et al., 1999; Jornvall et al., 2004). In the wt embryo, *Cryptic* is expressed in the anterior and lateral mesoderm (Fig. 5a). In *Cripto*$^{-/-}$ mutants, due to gastrulation failure, the mesoderm does not migrate and is not correctly specified; however, it is possible to detect the expression of *Cryptic* in this defective mesoderm, localized close to the extraembryonic region ($n=6$) (Fig. 5b). In *Cer1; Cripto* double mutants, *Cryptic* expression is even more reduced ($n=4$) (Fig. 5c). In addition, we could not detect any signal for *Alk7*, either in wt, *Cripto*$^{-/-}$ ($n=4$) or *Cer1;Cripto* ($n=5$) embryos (Figs. 5d–f). Thus, neither *Cryptic* nor *Alk7* expression appears significantly upregulated in the double mutants relative to the *Cripto*$^{-/-}$ embryos, in a manner that might compensate for the lack of Cripto. Finally, since Cer1 is also a Bmp4 inhibitor, we have analyzed by WISH the expression of *Bmp4* at both 6.7 (Figs. 5g–i) and 7.5 dpc (Figs. 5j–l). At both stages, we could not detect any difference in *Bmp4* expression among wt, *Cripto*$^{-/-}$ ($n=9$) and *Cer1; Cripto* ($n=8$) mutants. These data suggest first that the Bmp4 pathway is not directly implicated in *Cer1;Cripto* recovery and second that extraembryonic ectoderm (which is fundamental to restrict AVE induction to the distal tip and to initiate its migration anteriorward; Rodriguez et al., 2005) is specified normally in the *Cer1;Cripto* double mutants.

Another factor that could be involved in the signaling activity responsible for the rescue is the TGF-β factor Gdf1. It has been recently described that Gdf1 and Nodal interact during mouse development, and that these signals are preferentially transduced through ALK4 and not ALK7 (Andersson et al., 2006). In our *Cer1;Cripto* double mutant model, Gdf1 is unlikely to compensate for Nodal in the initial A–P axis positioning since it was shown to be expressed only after 7.0 dpc. *Gdf1* null mutants undergo normal gastrulation (Rankin et al., 2000) and Gdf1 cooperates with Nodal in midline development but not for A–P axis positioning (Andersson et al., 2006). Another recently identified member of the TGF-β superfamily, *Gdf3*, is expressed during early development, and is essential for AVE induction and A–P axis positioning (Chen

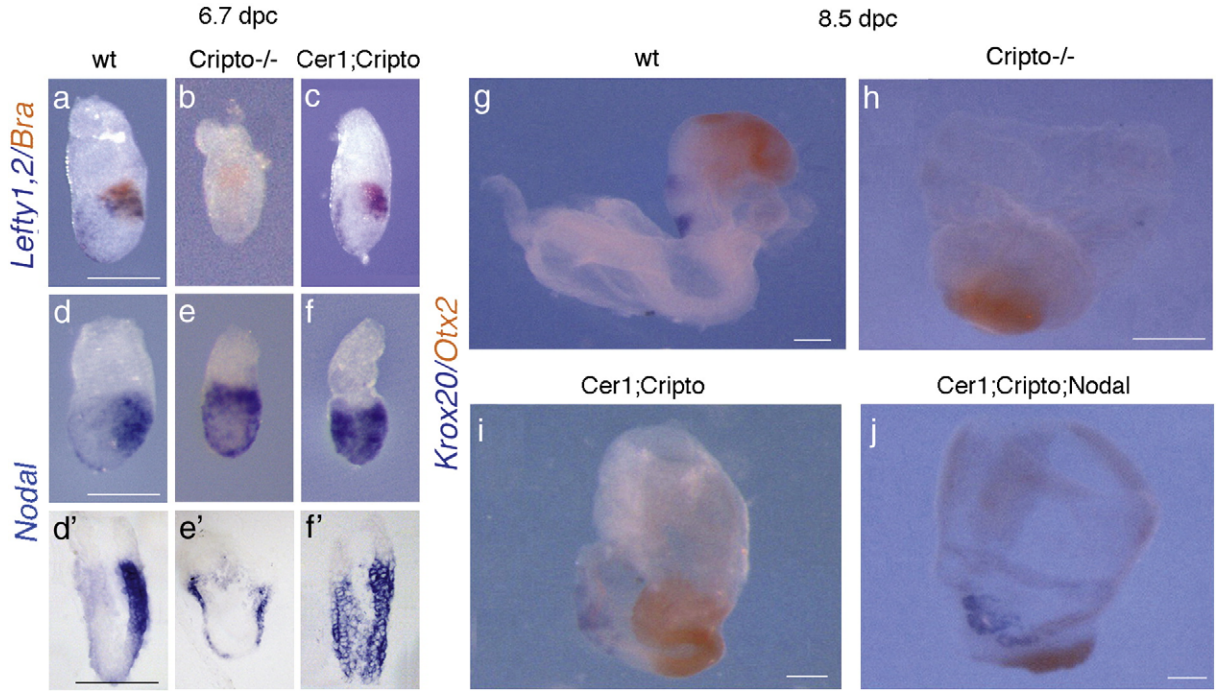

Fig. 4. The rescue observed in *Cer1;Cripto* double mutants is due to a recovery of *Nodal* signaling. Molecular analysis by double whole-mount *in situ* hybridization (WISH) of 6.7 dpc (a–f) and 8.5 dpc (g–j) wild-type (wt) (a, d, g), *Cripto*$^{-/-}$ (b, e, h), *Cer1;Cripto* (c, f, i) and *Cer1;Cripto;Nodal* embryos (j). After hybridization with *Nodal* probe wt (d′), *Cripto*$^{-/-}$ (e′) and *Cer1;Cripto* (f′) embryos were sectioned. All the sections are sagittal. (a–c) In the wt embryo *Brachyury* (red) is expressed in the PS, while *Lefty1* is detected in the AVE and *Lefty2* in the PS (both genes in blue) (a). *Cripto*$^{-/-}$ embryos lack expression of *Lefty* genes (b), while *Cer1;Cripto* embryos show rescue of the expression and the localization of both *Lefty1* and *Lefty2* (c). (d–f and d′–f′) *Nodal* is expressed in the AVE and in the posterior epiblast of the wt embryo (d, d′) and is detected in the VE and only in a proximal ring of epiblast cells of the *Cripto*$^{-/-}$ embryos (e, e′). *Cer1;Cripto* double mutants express *Nodal* in almost the entire epiblast (f–f′). (g–k) Double WISH for *Krox20* (blue) and *Otx2* (red) in wt (g), *Cripto*$^{-/-}$ (h), *Cer1;Cripto* double mutant (i) and *Cer1;Cripto; Nodal* triple mutant embryos (j). Reduction of Nodal gene dosage impairs the amount of rescue in *Cer1;Cripto* double mutants. Scale bars represent 300 μm.

et al., 2006; Levine and Brivanlou, 2006). However, its signaling activity was shown to be Cripto-dependent, being unlikely to compensate for the lack of Nodal signaling in the *Cripto*$^{-/-}$ animals and therefore, in our own experiments (Chen et al., 2006; Levine and Brivanlou, 2006). Nevertheless we cannot discard the involvement of additional signaling molecules, possibly novel TGF-β related signals that may also cooperate with Nodal during early development.

Cripto-independent Nodal signaling guides positioning of the A–P axis

Regional differences in signaling are instrumental in directing the movement of visceral endoderm cells (reviewed in Tam et al., 2006). Nodal signaling and the regionalization of its antagonists are required for normal migration of the prospective AVE from the distal tip of the embryo to the anterior side (Yamamoto et al., 2004). Whereas Nodal activity provides the driving force for AVE migration by stimulating the proliferation of visceral endoderm cells, the antagonists Cer1 and Lefty1 determine the direction of migration by asymmetric inhibition of Nodal activity on the future anterior (Yamamoto et al., 2004). The loss of only one of the two inhibitors does not affect AVE migration and gastrulation, while the inhibition of both *Cer1* and *Lefty1* genes causes marked expansion of *Hex* expression domain in the AVE, delayed migration of AVE cells and also formation of multiple primitive streaks (Belo et al., 2000; Meno et al., 1998; Perea-Gomez et al., 2002; Yamamoto et al., 2004). These data indicate functional redundancy between *Cer1* and *Lefty1* in the formation of the A–P axis (Perea-Gomez et al., 2002; Yamamoto et al., 2004). Here we report that, in the *Cer1;Cripto* double mutants, AVE migration to the prospective anterior is significantly rescued compared to the *Cripto* single mutants. In agreement with the model proposed by Yamamoto and coworkers (2004), we find that *Cer1;Cripto* double mutants, in contrast to *Cripto*$^{-/-}$ embryos, recover Nodal signaling and express *Lefty1* gene in the AVE. This suggests that the asymmetry in Nodal activity required for AVE migration is achieved in the *Cer1;Cripto* double mutants. Canonical Wnt signaling and its antagonist also regulate A–P axis polarization (Kimura-Yoshida et al., 2005). Wnt3 and Dkk function as repulsive and attractive guidance cues, respectively, in the migration of visceral endoderm cells (Kimura-Yoshida et al., 2005). Recent data on the crosstalk between Nodal and Wnt

Table 1
Percentage of phenotypic rescue observed in the *Cerl1;Cripto* versus the *Cerl1;Cripto;Nodal* mutant embryos

Genotype	Rescue of *Krox20* expression	%
Cerl1$^{+/-}$;*Cripto*$^{-/-}$ *Cerl1*$^{-/-}$;*Cripto*$^{-/-}$	46/78 (n=78)	59
Cerl1$^{+/-}$;*Cripto*$^{-/-}$;*Nodal*$^{+/-}$ *Cerl1*$^{-/-}$;*Cripto*$^{-/-}$;*Nodal*$^{+/-}$	5/20 (n=20)	25

P<0.01.

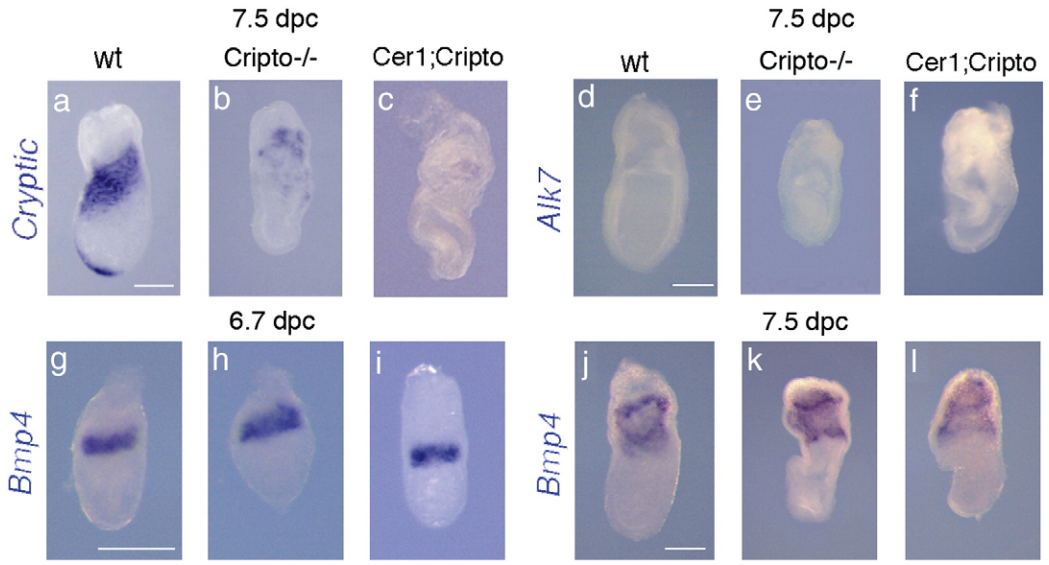

Fig. 5. Expression profiles of others genes involved the in Nodal pathway. (a–c) *cryptic* expression in the anterior and lateral mesoderm of the wt embryo (a), in the defective mesoderm close to the extraembryonic region of *Cripto*$^{-/-}$ (b) and *Cer1;Cripto* mutants (c). (d–f) Alk7 expression is not detect either in wt (d), *Cripto*$^{-/-}$ (e) and *Cer1;Cripto* (f) embryos. (g–l) Expression of *Bmp4* at both 6.7 (g–i) and 7.5 dpc (j–l). At 6.7 dpc, *Bmp4* is expressed in the extraembryonic ectoderm immediately adjacent to the epiblast of wt embryo (g), as well as in both *Cripto* null (h) and *Cer1;Cripto* double (i) mutants. At 7.5 dpc, *Bmp4* is also expressed in the extraembryonic mesoderm, without any significant difference among wt, *Cripto*$^{-/-}$ and *Cer1;cri* embryos (j–l). Scale bars represent 300 μm.

pathways suggest that *Wnt3* is induced by Nodal in a Cripto-independent manner (Ben-Haim et al., 2006). In agreement with these data, the *Cripto* single mutants still express *Wnt3*, even though its expression is fainter than in wt embryo and stays as a ring in the proximal region of the embryo. Concomitantly, *Dkk* expression, which marks the AVE, has been detected in the distal visceral endoderm of *Cripto*$^{-/-}$ embryos. By contrast, *Cer1;Cripto* double mutants show *Wnt3* expression shifted toward the posterior of the embryo and *Dkk* expression toward the anterior, even though *Wnt3* expression remains as weak as in the *Cripto* single mutants. These data indicate that both *Cripto*$^{-/-}$ and *Cer1;Cripto* mutants show an asymmetric distribution of Wnt3 ligand and its antagonist Dkk. However, in the double mutants at 6.7 dpc, this asymmetry is more oriented along the A–P axis. This is not accompanied by an increase in *Wnt3* expression with respect to *Cripto* single mutants, suggesting that Wnt3 signaling is not the driving force responsible for axial rotation in the *Cer1;Cripto* double mutants.

Cripto-independent Nodal signaling is inhibited by Cer1

Although Cripto has been presented as an essential coreceptor for Nodal signaling, the mouse *Cripto* null mutation does not precisely phenocopy the *Nodal* loss of function, being instead less severe (Brennan et al., 2001; Conlon et al., 1994; Ding et al., 1998; Liguori et al., 2003). These data indicate that, in the mouse embryo, Nodal signals through both Cripto-dependent and independent pathways. Recent data have highlighted an early role of Nodal activity in specifying embryonic visceral endoderm and elongating the egg cylinder, before inducing prospective AVE and germ layer formation (Mesnard et al., 2006). On the other side, we report that in the mouse embryo Cripto-independent Nodal signaling is able to orient the A–P axis properly and to form both anterior mesendoderm and posterior neuroectoderm. Our data, together with that of Mesnard and coworkers (2006), strengthen the difference between Nodal and Cripto requirements in the mouse embryo and put in evidence an increasing amount of Nodal functions that do not absolutely require Cripto. Moreover, our data suggest that removal of Cer1 is able to activate Cripto-independent Nodal signaling. We hypothesize that two different Nodal pathways are active in the early mouse embryo: one that is Cripto-dependent and the other that is Cripto-independent, the latter remaining active until *Cer1* expression.

Our hypothesis provides an adequate explanation for the phenotype of both *Cripto* single mutants and *Cer1;Cripto* double mutants. In fact, in the *Cripto* null mutants, the prospective AVE forms and expresses *Cer1*, but then fails to move anteriorward. The initial specification of the AVE would thus be due to Cripto-independent Nodal signaling. Subsequently, when Cer1 starts to be expressed, it inhibits the Cripto-independent pathway; the resulting absence of a Nodal signaling affects both the anterior AVE movement and gastrulation. In the *Cer1;Cripto* mutants, the Cripto-dependent pathway is severely compromised, just as in the *Cripto* single mutants. However, as a consequence of *Cer1* reduction or loss-of-function, the Cripto-independent pathway remains active and is able to mediate not only AVE formation as in the Cripto single mutants, but also the complete positioning of the A–P axis as well as formation of the mesendoderm.

It is tempting to speculate on how Cer1 might affect the Cripto-independent Nodal pathway. Ben-Haim et al. (2006) have recently generated a mouse model producing a mutant Nodal precursor that is resistant to cleavage and processing but which apparently can still signal. One possibility is thus that

Cer1 might antagonize such a Nodal precursor, either by directly blocking its activity or by altering its stability and/or diffusion; loss of Cer1 activity would thus lead to an increase in Nodal precursor signaling. However, at 6.5 dpb, Cer1 is not expressed in mutants defective in Nodal processing (Beck et al., 2002; Ben-Haim et al., 2006), making this model an unlikely explanation for the phenotypic rescue observed in the *Cer1; Cripto* double mutants.

In conclusion, our data suggest the existence of Cripto-independent signaling mechanisms, by which Nodal controls axis specification and initiates gastrulation in the early mouse embryo. These mechanisms are inhibited by Cer1. In principle, Cer1 could antagonize Nodal protein by two (non-exclusive) mechanism: by blocking Nodal ligand directly and decreasing Nodal signaling activity or by acting on specific components of the Cripto-independent pathway. Interestingly, a dual role as Nodal antagonist has also been described for Lefty (Chen and Shen, 2004). Such scenarios in which different antagonists act on different players in Nodal signaling pathways point to additional levels of complexity within the Nodal regulatory network.

Acknowledgments

We thank M.R. Kuehn for *Nodal* mutants; J.C. Izpisúa-Belmonte, S. Filosa, H. Hamada and A. Simeone for probes; Tania Moccia and Maria Terracciano for technical assistance; Luca D'Orsi, Ivan Solombrino and both the "G. Pascale" and the IGC Animal Facility for animal care. We thank J. McGhee, V. Teixeira, A. Tavares. M. Ciullo, D. Constam and S. Filosa for critically reading of this manuscript. A.C. Borges, L. Gonçalves and A.M. Salgueiro are recipient of F.C.T. (SFRH/BD/3214/2000 and SFRH/BPD/20576/2004 to A.C.B.; SFRH/BD/21924/2005 to L.G.) and IEFP fellowships. G.L. Liguori and A.C. Borges were also supported by CNR/GRICES. D. D'Andrea was supported by FIRC fellowship. This work was supported by grants from the FIRB and AIRC to M.G. Persico and by grants from F.C.T. and IGC/Fundação Calouste Gulbenkian to J.A. Belo.

References

Adkins, H.B., Bianco, C., Schiffer, S.G., Rayhorn, P., Zafari, M., Cheung, A.E., Orozco, O., Olson, D., De Luca, A., Chen, L.L., Miatkowski, K., Benjamin, C., Normanno, N., Williams, K.P., Jarpe, M., LePage, D., Salomon, D., Sanicola, M., 2003. Antibody blockade of the Cripto CFC domain suppresses tumor cell growth in vivo. J. Clin. Invest. 112, 575–587.

Andersson, O., Reissmann, E., Jornvall, H., Ibanez, C.F., 2006. Synergistic interaction between Gdf1 and Nodal during anterior axis development. Dev. Biol. 15, 370–381.

Ang, S.L., Constam, D.B., 2004. A gene network establishing polarity in the early mouse embryo. Semin. Cell Dev. Biol. 15, 555–561.

Beddington, R.S.P., 1998. Cripto-analysis of embryonic codes. Nature 395, 641–643.

Beddington, R.S.P., Robertson, E.J., 1998. Anterior patterning in the mouse. Trends Genet. 14, 277–284.

Beddington, R.S.P., Robertson, E.J., 1999. Axis development and early asymmetry in mammals. Cell 96, 195–209.

Belo, J.A., Bouwmeester, T., Leyns, L., Kertesz, N., Gallo, M., De Robertis, E.M., 1997. Cerberus-like is a secreted factor with neuralizing activity expressed in the anterior primitive streak endoderm of the mouse gastrula. Mech. Dev. 68, 45–57.

Belo, J.A., Bachiller, D., Agius, E., Borges, A.C., Marques, S., Piccolo, S., De Robertis, E.M., 2000. Cerberus-like is a secreted BMP and Nodal antagonist not essential for mouse development. Genesis 26, 265–270.

Ben-Haim, N., Lu, C., Guzman-Ayala, M., Pescatore, L., Mesnard, D., Bischofberger, M., Naef, F., Robertson, E.J., Constam, D.B., 2006. The Nodal precursor acting via activin receptors induces mesoderm by maintaining a source of its convertases and BMP4. Dev. Cell 11, 313–323.

Bianco, C., Strizzi, L., Rehman, A., Normanno, N., Wechselberger, C., Sun, Y., Khan, N., Hirota, M., Adkins, H., Williams, K., Margolis, R.U., Sanicola, M., Salomon, D.S., 2003. A Nodal- and ALK4-independent signaling pathway activated by Cripto-1 through Glypican-1 and c-Src. Cancer Res. 63, 1192–1197.

Beck, S., Le Good, J.A., Guzman, M., Ben Haim, N., Roy, K., Beermann, F., Constam, D.B., 2002. Extraembryonic proteases regulate Nodal signalling during gastrulation. Nat. Cell Biol. 4, 981–985.

Brennan, J., Lu, C.C., Norris, D.P., Rodriguez, T.A., Beddington, R.S., Robertson, E.J., 2001. Nodal signalling in the epiblast patterns the early mouse embryo. Nature 411, 965–969.

Chen, C., Shen, M.M., 2004. Two modes by which Lefty proteins inhibit Nodal signaling. Curr. Biol. 14, 618–624.

Chen, C., Ware, S.M., Sato, A., Houston-Hawkins, D., Habas, R., Matzuk, M.M., Shen, M.M., Brown, W.C., 2006. The Vg1-related protein Gdf3 acts in a Nodal signalling pathway in the pre-gastrulation mouse embryo. Development 133, 319–329.

Cheng, S.K., Olale, F., Bennett, J.T., Brivanlou, A.H., Schier, A.F., 2003. EGF-CFC proteins are essential coreceptors for the TGF-beta signals Vg1 and GDF1. Genes Dev. 17, 31–36.

Cheng, S.K., Olale, F., Brivanlou, A.H., Schier, A.F., 2004. Lefty blocks a subset of TGFbeta signals by antagonizing EGF-CFC coreceptors. PLoS Biol. 2, 215–226.

Chu, J., Ding, J., Jeays-Ward, K., Price, S.M., Placzek, M., Shen, M.M., 2005. Non-cell-autonomous role for Cripto in axial midline formation during vertebrate embryogenesis. Development 132, 5539–5551.

Conlon, F.L., Lyons, K.M., Takaesu, N., Barth, K.S., Kispert, A., Herrmann, B., Robertson, E.J., 1994. A primary requirement for Nodal in the formation and maintenance of the primitive streak in the mouse. Development 120, 1919–1928.

Ding, J., Yang, L., Yan, Y.T., Chen, A., Desai, N., Wynshjaw-Boris, A., Shen, M.M., 1998. Cripto is required for correct orientation of the anterior–posterior axis in the mouse embryo. Nature 395, 702–707.

Gray, P.C., Harrison, C.A., Vale, W., 2003. Cripto forms a complex with activin and type II activin receptors and can block activin signaling. Proc. Natl. Acad. Sci. U. S. A. 100, 5193–5198.

Gray, P.C., Shani, G., Aung, K., Kelber, J., Vale, W., 2006. Cripto binds transforming growth factor beta (TGF-beta) and inhibits TGF-beta signaling. Mol. Cell. Biol. 26, 9268–9278.

Gritsman, K., Zhang, J., Cheng, S., Heckscher, E., Talbot, W.S., Schier, A.F., 1999. The EGF-CFC protein one-eye-pinhead is essential for Nodal signalling. Cell 97, 121–132.

Harms, P.W., Chang, C., 2003. Tomoregulin-1 (TMEFF1) inhibits Nodal signaling through direct binding to the Nodal coreceptor Cripto. Genes Dev. 17, 2624–2629.

Jornvall, H., Reissmann, E., Andersson, O., Mehrkash, M., Ibanez, C.F., 2004. ALK7, a receptor for Nodal, is dispensable for embryogenesis and left–right patterning in the mouse. Mol. Cell. Biol. 24, 9383–9389.

Kimura, C., Shen, M.M., Takeda, N., Aizawa, S., Matsuo, I., 2001. Complementary functions of Otx2 and Cripto in initial patterning of mouse epiblast. Dev. Biol. 235, 12–32.

Kimura-Yoshida, C., Nakano, H., Okamura, D., Nakao, K., Yonemura, S., Belo, J.A., Aizawa, S., Matsui, Y., Matsuo, I., 2005. Canonical Wnt signaling and its antagonist regulate anterior-posterior axis polarization by guiding cell migration in mouse visceral endoderm. Dev. Cell 9, 639–650.

Levine, A., Brivanlou, A.H., 2006. GDF3, a BMP inhibitor, regulates cell fate in stem cells and early embryos. Development 133, 209–216.

Liguori, G., Echevarria, D., Improta, R., Signore, M., Adamsom, E., Martinez, S., Persico, M.G., 2003. Anterior neural plate regionalization in Cripto null mutant mouse embryos in the absence of node and primitive streak. Dev. Biol. 264, 537–549.

Lowe, L., Yamada, S., Kuehn, M.R., 2001. Genetic dissection of Nodal function in patterning the mouse embryo. Development 128, 1831–1843.

Lu, C.C., Robertson, E.J., 2004. Multiple roles for Nodal in the epiblast of the mouse embryo in the establishment of anterior–posterior patterning. Dev. Biol. 273, 149–159.

Meno, C., Ito, Y., Saijoh, Y., Matsuda, Y., Tashiro, K., Kuhara, S., Hamada, H., 1997. Two closely-related left–right asymmetrically expressed genes, lefty-1 and lefty-2: their distinct expression domains, chromosomal linkage and direct neuralizing activity in *Xenopus* embryos. Genes Cells 2, 513–524.

Meno, C., Shimono, A., Saijoh, Y., Yashiro, K., Mochida, K., Ohishi, S., Noji, S., Kondoh, H., Hamada, H., 1998. lefty-1 is required for left–right determination as a regulator of lefty-2 and Nodal. Cell 94, 287–297.

Mesnard, D., Guzman-Ayala, M., Constam, D.B., 2006. Nodal specifies embryonic visceral endoderm and sustains pluripotent cells in the epiblast before overt axial patterning. Development 133, 2497–2505.

Norris, D.P., Brennan, J., Bikoff, E.K., Robertson, E.J., 2002. The FoxH1-dependent autoregulatory enhancer controls the level of Nodal signals in the mouse embryo. Development 129, 3455–3468.

Perea-Gomez, A., Vella, F.D.J., Shawlot, W., Oulad-Abdelghani, M., Chazaud, C., Meno, C., Pfister, V., Chen, L., Robertson, E.J., Hamada, H., Behringer, R.R., Ang, S.L., 2002. Nodal antagonists in the anterior visceral endoderm prevent the formation of multiple primitive streaks. Dev. Cell 3, 745–756.

Persico, M.G., Liguori, G., Parisi, S., D'Andrea, D., Minchiotti, G., 2001. Cripto in tumors and embryo development. Biochim. Biophys. Acta 1552, 87–93.

Rankin, C.T., Bunton, T., Lawler, A.M., Lee, S.J., 2000. Regulation of left–right patterning in mice by growth/differentiation factor-1. Nat. Genet. 24, 262–265.

Reissman, E., Jornvall, H., Blokzijl, A., Andersson, O., Chang, C., Minchiotti, G., Persico, M.G., Ibanez, C., Brivanlou, A., 2001. The orphan receptor ALK7 and the activin receptor ALK4 mediate signalling by Nodal proteins during vertebrate development. Genes Dev. 15, 2010–2022.

Rodriguez, T.A., Srinivas, S., Clements, M., P., Smith, J., C., Beddington, R., S., 2005. Induction and migration of the anterior visceral endoderm is regulated by the extra-embryonic ectoderm. Development 132, 2513–2520.

Schier, A.F., 2003. Nodal signalling in vertebrate development. Annu. Rev. Cell Dev. Biol. 19, 589–621.

Shen, M., M., 2007. Nodal signaling: developmental roles and regulation. Development 134, 1023–1034.

Shen, M.M., Schier, A.F., 2000. The EGF-CFC gene family in vertebrate development. Trends Genet. 16, 303–309.

Shen, M.M., Wang, H., Leder, P., 1997. A differential display strategy identifies cryptic, a novel EGF related gene expressed in the axial mesoderm during mouse gastrulation. Development 124, 429–442.

Song, J., Oh, S.P., Schrewe, H., Nomura, M., Lei, H., Okano, M., Gridley, T., Li, E., 1999. The type II activin receptors are essential for egg cylinder growth, gastrulation, and rostral head development in mice. Dev. Biol. 213, 157–169.

Strizzi, L., Bianco, C., Normanno, N., Salomon, D., 2005. Cripto-1: a multifunctional modulator during embryogenesis and oncogenesis. Oncogene 24, 5731–5741.

Tam, P.P., Loebel, D.A., Tanaka, S.S., 2006. Building the mouse gastrula: signals, asymmetry and lineages. Curr. Opin. Genet. Dev. 16, 419–425.

Varlet, I., Collignon, J., Robertson, E.J., 1997. Nodal expression in the primitive endoderm is required for specification of the anterior axis during mouse gastrulation. Development 124, 1033–1044.

Whitman, M., 2001. Nodal signaling in early vertebrate embryos: themes and variations. Dev. Cell 1, 605–617.

Xu, C., Liguori, G.L., Persico, M.G., Adamsom, E.D., 1999. Abrogation of Cripto gene in mouse leads to failure of postgastrulation morphogenesis and lack of differentiation of cardiomyocytes. Development 126, 483–494.

Yamamoto, M., Saijoh, Y., Perea-Gomez, A., Shawlot, W., Behringer, R.R., Ang, S.L., Hamada, H., Meno, C., 2004. Nodal antagonists regulate formation of the anteroposterior axis of the mouse embryo. Nature 428, 387–392.

Yan, Y.T., Gritsman, K., Ding, J., Burdine, R.D., Corrales, J.D., Price, S.M., Talbot, W.S., Schier, A.F., Shen, M.M., 1999. Conserved requirement for EGF-CFC genes in vertebrate left–right axis formation. Genes Dev. 13, 2527–2537.

Yan, Y.T., Liu, J.J., Luo, Y., E.C., Haltiwanger, R.S., Abate-Shen, C., Shen, M.M., 2002. Dual roles of Cripto as a ligand and coreceptor in the Nodal signaling pathway. Mol. Cell. Biol. 22, 4439–4449.

Yeo, C., Whitman, M., 2001. Nodal signals to Smads through Cripto-dependent and Cripto-independent mechanisms. Mol. Cell 7, 949–957.